

Redox-Responsive Polycondensate Neoepitope for Enhanced Personalized Cancer Vaccine

Lixia Wei,[§] Yu Zhao,[§] Xiaomeng Hu, and Li Tang*



Cite This: *ACS Cent. Sci.* 2020, 6, 404–412



Read Online

ACCESS |



Metrics & More

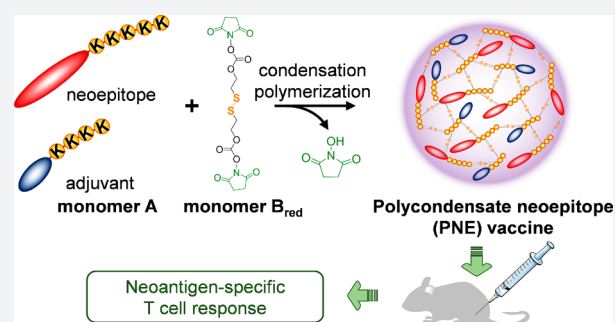


Article Recommendations



Supporting Information

ABSTRACT: A versatile and highly effective platform remains a major challenge in the development of personalized cancer vaccines. Here, we devised a redox-responsive polycondensate neoepitope (PNE) through a reversible polycondensation reaction of peptide neoantigens and adjuvants together with a tracelessly responsive linker-monomer. Peptide-based neoantigens with diverse sequences and structures could be copolymerized with molecular adjuvants to form PNEs of high loading capacity for vaccine delivery without adding any carriers. The redox-responsive PNEs with controlled molecular weights and sizes efficiently targeted and accumulated in draining lymph nodes and greatly promoted the antigen capture and cross-presentation by professional antigen presenting cells. Mice immunized with PNEs showed markedly enhanced antigen-specific T cell response and the protective immunity against the tumor cell challenge.



INTRODUCTION

Therapeutic cancer vaccines designed to induce or augment anticancer T cell responses have shown clinical benefits in many phase I/II studies.¹ However, the clinical efficacy of cancer vaccines remains modest in comparison with other immunotherapies such as checkpoint blockades and adoptive T cell therapies.² Cancer vaccines targeting antigens derived from random somatic mutations in tumor cells but not present in normal cells, termed neoantigens, have recently been developed as a personalized immunotherapy and shown great promise in the treatment of late-stage melanoma.^{3–5} Compared to self-antigens, neoantigens could be recognized as nonself by the host immune system and are thus attractive targets for immunotherapies with potentially increased specificity, efficacy, and safety.^{6–8} However, the elicited anticancer T cell response by current neoantigen-based vaccines is in general weak and short-lived partially due to the lack of a versatile and highly effective delivery platform that can be readily adapted for vastly diverse neoepitopes identified from individual patients.

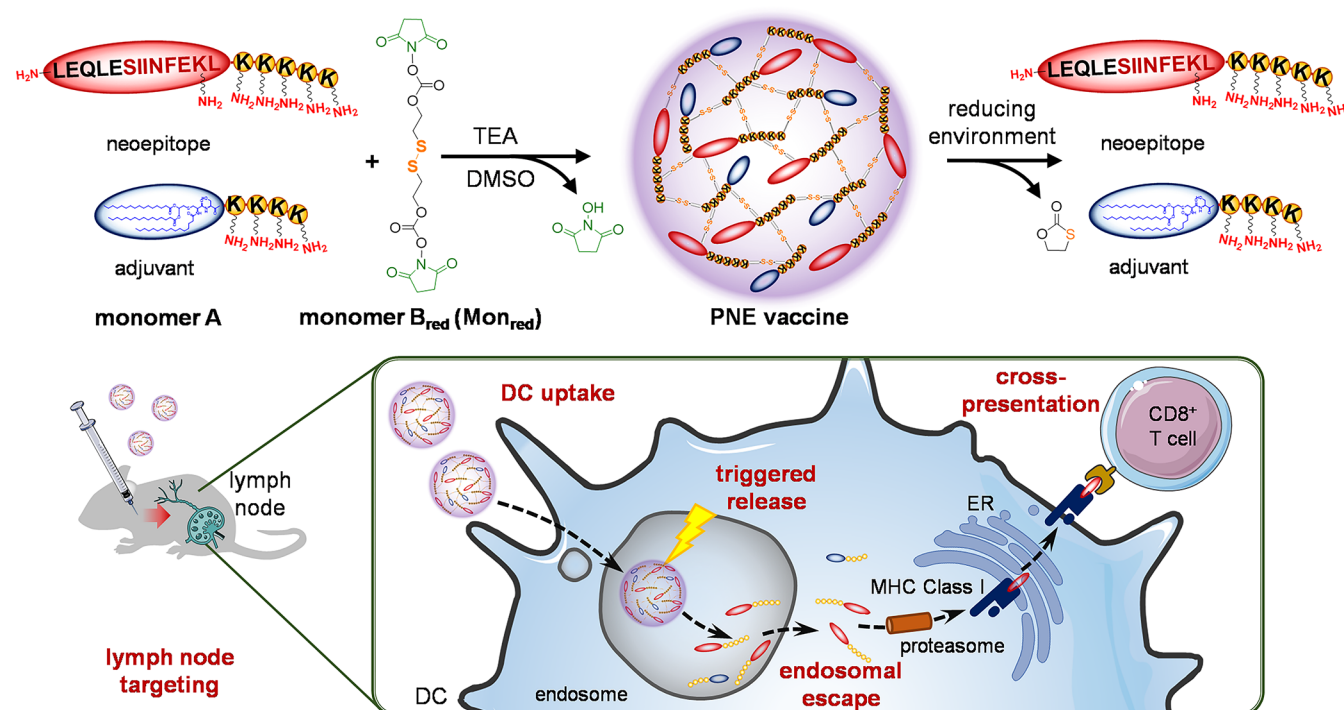
Synthetic peptide is the most commonly used form of neoepitopes in cancer vaccines given its direct function as pivotal T cell epitope with high efficiency of antigen processing by antigen presenting cells (APCs),^{9,10} low cost, ease of synthesis, and good stability *in vivo*.¹¹ However, there are two major challenges in the delivery of peptide-based cancer vaccines. One is targeting antigens in tandem with suitable adjuvants to secondary lymphoid organs, such as lymph nodes (LNs), to facilitate robust antigen capture and processing by professional APCs, such as dendritic cells (DCs). Parenterally injected soluble peptide antigens or adjuvant molecules quickly disseminate into the systemic circulation due to the small sizes

and show very poor accumulation in LNs leading to limited immune responses.^{12,13} Moreover, soluble molecular adjuvants administered subcutaneously often result in significant local or systemic inflammatory toxicities.¹⁴ Another major challenge in cancer vaccine delivery is to elicit robust cytotoxic CD8⁺ T cell responses, which are essential for eradicating tumor cells through orchestrating with CD4⁺ T cell responses.^{15,16} Soluble subunit antigens acquired by DCs from the extracellular environment are internalized into endolysosomal compartments and loaded almost exclusively onto major histocompatibility complex (MHC) class II molecules for the presentation to CD4⁺ helper T cells. Typically, only antigens located in the cytosol can be loaded onto MHC class I molecules for the presentation to CD8⁺ killer T cells, a process termed cross-presentation.¹⁷ Thus, it is critical to control the intracellular pathways of captured antigens for enhanced cross-presentation.

Here, we demonstrate a new and versatile approach to address the major challenges in neoantigen cancer vaccine delivery by “polymerizing” the neoepitopes through a reversible polycondensation reaction. Using synthetic long peptide (SLP) bearing a neoepitope and multiple amino groups as one monomer (monomer A) mixed with another reactive bifunctional monomer (monomer B), we prepared a polycondensate neoepitope (PNE) with controlled sizes and responsiveness (Scheme 1), which showed superior LN targeting compared to

Received: November 13, 2019

Published: February 3, 2020

Scheme 1. Schematic Illustration of the Synthesis, Responsive Release, and *in Vivo* Fate of Polycondensate Neoepitope (PNE) Vaccines^a

^aDMSO, dimethylsulfoxide; TEA, triethylamine.

Table 1. Physicochemical Properties of PNE Vaccines

entry	PNE	monomer A		monomer B	size ^a (nm)
		antigen (epitope is underlined)	adjuvant		
1	PNE(LEQ)	LEQLESIIINFEKL ₅		Mon _{red}	8.14 ± 1.54
2	PNE(LEQ-Pam)	LEQLESIIINFEKL ₅	Pam ₃ CSK ₄	Mon _{red}	16.69 ± 3.14
3	Nondeg. PNE(LEQ-Pam)	LEQLESIIINFEKL ₅	Pam ₃ CSK ₄	Mon _{BS3} ^b	45.97 ± 5.70
4	PNE(LEQLEK ₅ -Pam)	LEQLEK ₅ AAYSIIINFEKL	Pam ₃ CSK ₄	Mon _{red}	13.62 ± 1.41
5	PNE(K ₅ LEQ-Pam)	K ₅ LEQLEAAYSIIINFEKL	Pam ₃ CSK ₄	Mon _{red}	21.32 ± 3.04
6	PNE(ELE-Pam)	ELEK ₅ AAYSMTNMELM	Pam ₃ CSK ₄	Mon _{red}	12.48 ± 1.06
7	PNE(CSV)	CSVYDFVWLK ₅		Mon _{red}	8.90 ± 1.10
8	PNE(CLC)	CLCPGNKYEMK ₅		Mon _{red}	7.40 ± 1.10
9	PNE(LEQ-CpG)	LEQLESIIINFEKL ₅	CpG ^c	Mon _{red}	24.97 ± 4.40

^aDiameters of the PNEs were characterized by DLS. ^bMon_{BS3}: bis(sulfosuccinimidyl)suberate. ^cAmino-functionalized CpG (5′/-5AmMC6/TCCATGACGTTCCCTGACGTT/3AmMO/-3).

monomeric SLP. Molecularly defined adjuvants, such as toll-like receptor (TLR) ligands that bear amino groups, were copolymerized for the codelivery with antigens to LNs for efficient activation of APCs. Upon internalization by APCs, PNE released neoepitopes rapidly in response to intracellular reduction activity facilitating the endosomal escape and cytosol delivery of peptide antigens and markedly promoted the cross-presentation. We found PNE elicited potent antigen-specific CD8⁺ T cell responses in immunized mice and expanded the effector memory CD8⁺ T (T_{EM}) cells to 22.8-fold greater number than the vaccine of equivalent dose delivered by Montanide emulsion (arguably the most potent vaccine adjuvant used in the clinic to date^{18–20}), therefore enabling markedly enhanced antitumor efficacy in a prophylactic mouse model.

RESULTS AND DISCUSSION

Molecular weight (MW) has been reported as a key factor that determines the passive distribution of proteins to blood circulation versus lymphatic circulation upon parenteral injections.^{21,22} Soluble peptide antigens and molecular adjuvants typically have MW < 5k Da and quickly get cleared into the systemic circulation due to the small sizes eliciting minimum immune responses.²³ In order to increase the MW and size to target lymphoid organs, we sought to copolymerize the SLP neoantigens and adjuvants through a reversible polycondensation reaction as illustrated in Scheme 1. To prove the concept, we first used a SLP containing SIINFEKL (SII), the CD8 epitope of ovalbumin (OVA), as a model neoantigen (LEQ, Table 1, entry 1; the detailed composition and reaction conditions are listed in Table S1), which was modified with multiple amino groups by adding flanking lysine residues (monomer A, Scheme 1). An amino-reactive bifunc-

tional monomer B bearing a disulfide and two *N*-hydroxysuccinimide (NHS) groups (Mon_{red}) was synthesized for the polycondensation reaction (Scheme 1; Figure S1). We first mixed monomer A (SLP only), and monomer B in anhydrous dimethyl sulfoxide (DMSO), to prepare the PNE with responsiveness to reduction activity. Triethylamine (TEA) was added as a catalyzer to initiate the polycondensation. The PNE(LEQ) polymer was successfully prepared as evidenced by broadened peaks as compared to the peptide monomer in a ¹H NMR spectrum (Figure S2) and MW increase shown in traces in ultra-high-performance liquid chromatography (UHPLC) equipped with a size-exclusion chromatography (SEC) column (Figure 1A). PNE(LEQ) exhibited an average hydrodynamic

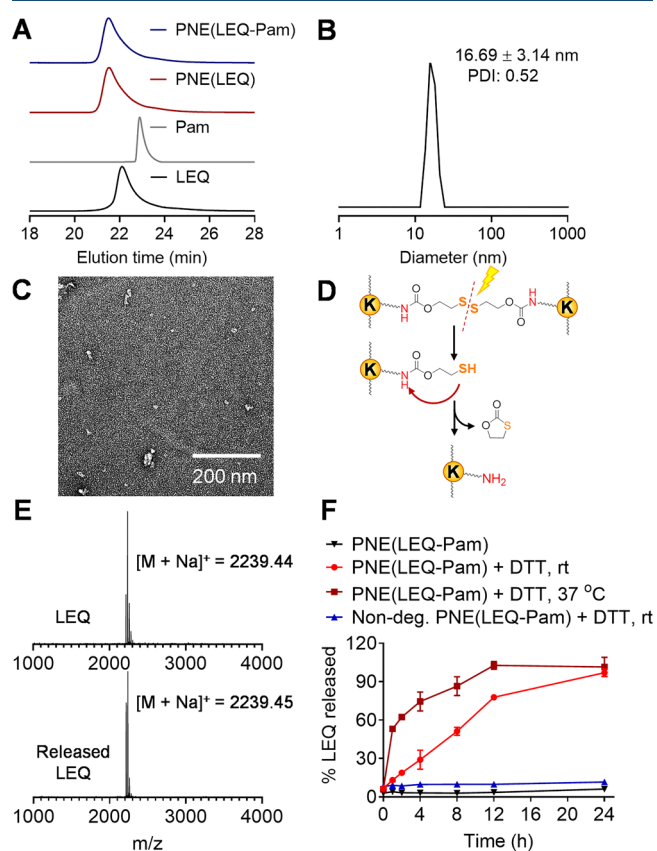


Figure 1. Characterizations of PNE vaccines. (A) UHPLC-SEC traces of LEQ, Pam, PNE(LEQ), and PNE(LEQ-Pam), detected by UV adsorption at a wavelength of 220 nm. (B) Size and size distribution measurement of PNE(LEQ-Pam) by DLS. (C) TEM imaging of PNE(LEQ-Pam). (D) Scheme of the redox-responsive release of antigens or adjuvants from PNE(LEQ-Pam). (E) Matrix-assisted laser desorption/ionization time-of-flight (MALDI-TOF) mass spectrometric analysis of native and released LEQ from PNE(LEQ-Pam). (F) Release kinetics of LEQ from PNEs in the presence or absence of a reducing agent DTT (2 mM).

diameter of 8.14 ± 1.54 nm characterized by dynamic light scattering (DLS) and transmission electron microscopy (TEM) (Table 1, entry 1; Table S1, entry 1; Figure S3).

Codelivery of antigens and adjuvants to the same endosomal/phagosomal compartment of an APC has been shown to be essential for physically instructing DCs to present the foreign antigens.²⁴ We next copolymerized LEQ and Pam₃CSK₄ (Pam), a TLR1/2 agonist as a molecular adjuvant, with Mon_{red} forming a self-adjuvanted PNE(LEQ-Pam) (Scheme 1). Pam was

selected as it bears multiple amino groups facilitating the direct polycondensation with Mon_{red} and has been shown to potentially amplify T cell priming when conjugated with peptides.^{25–28} PNE(LEQ-Pam) showed increased MW compared to the monomers as observed in both characterizations of UHPLC-SEC (Figure 1A) and gel permeation chromatography (GPC) (Figure S4A) suggesting the successful copolymerization. Further, a negligible amount of both monomers (LEQ and Pam) was detected by HPLC equipped with a C18 column (Figure S4B,C) or sodium dodecyl sulfate-polyacrylamide gel electrophoresis (SDS-PAGE) (Figure S5) indicating a quantitative monomer conversion. Together, >99% incorporation efficiency and remarkably high loading capacity of cargos (~46.4% of dry weight was LEQ, and 7.9% was Pam, Table S1, entry 2) have been achieved with the PNE platform. In addition, the as-prepared PNE(LEQ-Pam) had a relatively homogeneous size with a mean hydrodynamic diameter of 16.69 ± 3.14 nm (Table 1, entry 2; Figure 1B,C)

PNE was designed to be degraded in response to intracellular reduction activity facilitating a traceless release of intact peptide antigens through a self-immolative reaction (Scheme 1; Figure 1D) for unaltered processing and presentation of the designed subunit antigens. Released LEQ peptide from PNE(LEQ-Pam) shared the same MW as the original LEQ peptide providing the evidence of releasing unmodified peptide antigens without any residue chemical groups (Figure 1E). Consistent with the expectations, reducing agents, such as dithiothreitol (DTT), accelerated the release of LEQ from the PNE at both room temperature (rt) and 37 °C (Figure 1F), whereas PNE prepared with a nondegradable monomer B (nondeg. PNE(LEQ-Pam)) (Table 1, entry 3; Figure S6) showed no detectable release of antigens even in the presence of DTT. The intracellular traceless release of antigens could be important for the efficient antigen processing and presentation by DCs.²⁹

To test the versatility, we have extended the preparation of PNEs to a number of SLP antigens with diverse structures and properties including neoantigens identified from mouse tumors (Table 1; Table S1). In the design of those SLPs containing neoepitopes, the flanking sequence of negatively charged glutamic acid residues was added to balance the overall charge, and a proteolytic spacer (AAY) was added next to the epitope to ensure the correct antigen processing and presentation.³⁰ We found that the successful formation of PNEs was independent of the sequence or the position of flanking amino acids next to the epitope (Table 1, entries 2, 4, and 5), or the sequence of epitope itself (Table 1, entries 2 and 6–8; including neoantigens identified from MC38 murine colorectal cancer or B16F10 murine melanoma), or the adjuvant molecules (Table 1, entries 2 and 9; triacylated lipopeptide Pam can be replaced by amino-functionalized CpG oligodeoxynucleotide). Depending on the properties of SLP antigens and adjuvants, the PNE synthesis could be done in DMSO (Table S1, entries 1, 2, 5, and 6) or aqueous solution (Table S1, entries 3, 4, and 7–9). The amino group was chosen as the chemical handle for the polycondensation due to the ease of adding flanking lysines during the peptide synthesis without significantly changing the properties of SLPs. The amino-NHS conjugation-based polycondensation was rapid and highly efficient in DMSO or aqueous solution at ambient conditions providing PNE a highly versatile and potentially scalable platform for diverse epitopes.

We next investigated the targeting efficiency of the responsive PNEs to LNs. Free SLP, adjuvant, or the mixture of the two in the presence or absence of Montanide, or PNE(LEQ-Pam)

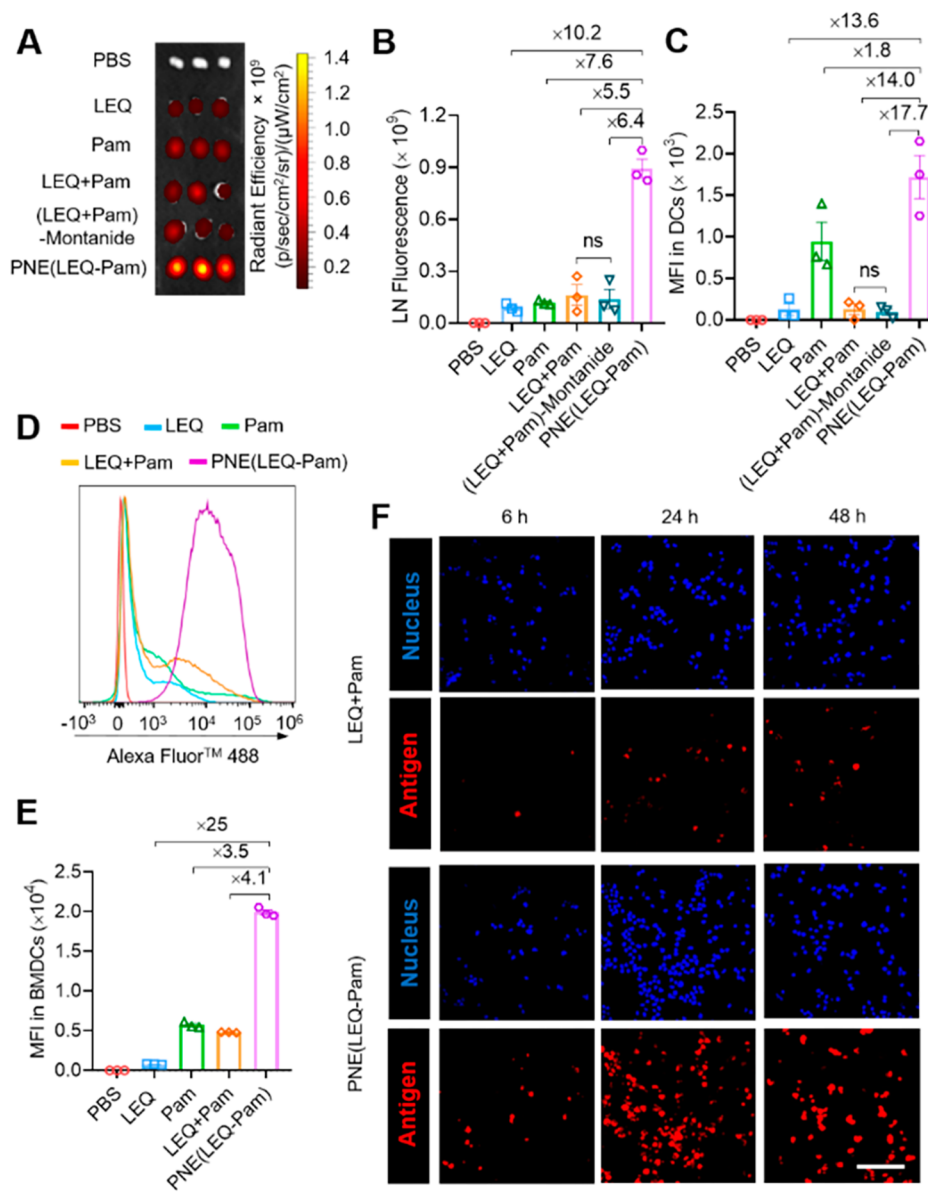


Figure 2. Lymph node (LN) and DC targeting of PNE(LEQ-Pam) vaccines *in vivo*. (A) IVIS fluorescence imaging and (B) quantification of inguinal LNs excised from mice treated with various vaccines. (C) MFI of fluorescence signal in vaccines that were internalized by DCs in the inguinal LNs. (D) Representative flow cytometry histograms of Alexa Fluor 488 labeled vaccines that were internalized by BMDCs. (E). MFI of internalized vaccine formulations by BMDCs. (F) Confocal microscopy images of BMDCs antigen uptake. Scale bar: 40 μ m.

labeled with equivalent amount of fluorescence dye Alexa Fluor 647 was injected subcutaneously into C57BL/6 mice at the tail base. Then, 24 h later, the draining LNs were excised for whole-tissue fluorescence imaging and measurement. Monomeric SLP or adjuvant or the simple mixture of the two showed limited accumulation in LNs (Figure 2A,B). The formulation of LEQ+Pam in Montanide ((LEQ+Pam)-Montanide) did not improve the LN targeting of the vaccine. By contrast, vaccine delivered by PNE exhibited remarkably high LN accumulation reaching a level that was 10.2-, 7.6-, and 5.5-fold greater than free SLP, adjuvant, and the simple mixture of the two, respectively. Additionally, PNE(LEQ) without adjuvant exhibited similar LN targeting ability as the one with adjuvant (Figure S7). The efficient and fast (within 24 h) LN targeting of PNE can be attributed to the well-controlled small size (~ 20 nm in diameter), which permits the rapid trafficking to lymphoid organs through the afferent lymph.^{13,22,31,32}

Next, we assessed the efficiency of antigen capture by the APCs in LNs using flow cytometry. DCs are critical APCs that efficiently process internalized antigens into peptide-MHC complexes (pMHC), which are required for eliciting T cell immune responses.^{9,33} PNE vaccine was captured efficiently by the DCs ($CD11c^+$) in LNs with 14.0- and 17.7-fold higher mean fluorescence intensity (MFI) than that of the mixture of free SLP and adjuvant in the absence or presence of Montanide, respectively (Figure 2C). The antigen capture was further examined *in vitro* with bone-marrow-derived dendritic cells (BMDCs). Similar to the *in vivo* results, PNE(LEQ-Pam) exhibited a substantially higher level of antigen internalization compared to the simple mixture LEQ+Pam (Figure 2D–F). Slightly higher DC internalization of free Pam compared to free LEQ was likely due to the fact that Pam could self-assemble into some nanosized structures. In general, nanovaccines are known to be internalized more efficiently by APCs than soluble subunit

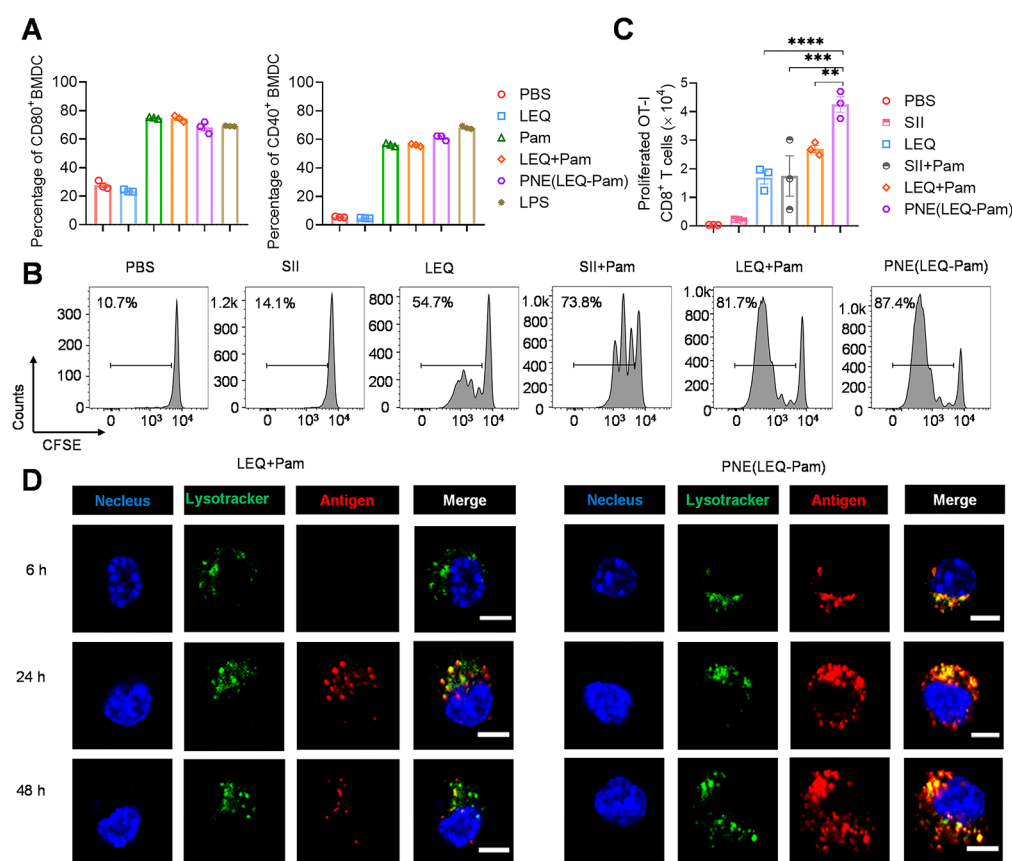


Figure 3. *In vitro* BMDC maturation and antigen cross-presentation. (A) Frequencies of BMDCs expressing maturation markers (CD80 and CD40) treated with PNE(LEQ-Pam) vaccine or other indicated formulations. (B) Representative flow cytometry plots showing CFSE dilution and gating of the proliferated OT-1 CD8⁺ T cells cocultured with BMDCs pulsed with PNE or other indicated formulations. Naïve OT-1 T cells were labeled with CFSE (1 μ M for 10 million cells) in the beginning of the assay. (C) Counts of proliferated OT-1 CD8⁺ T cells. * $P < 0.05$; ** $P < 0.01$; *** $P < 0.001$; **** $P < 0.0001$. (D) Confocal microscopic images of BMDCs incubated with fluorescently labeled PNE(LEQ-Pam) or the mixture of free LEQ and Pam. LEQ was labeled with Alexa Fluor 647 (red); the endolysosomes were stained with LysoTracker (green); the nuclei were stained with Hoechst (blue). Scale bar: 5 μ m.

vaccines.^{12,13} Together, PNE efficiently delivers neoantigen vaccines to LNs and DCs for antigen capture and presentation.

Next, we examined the impact of PNE platform on antigen presentation. DC maturation is critical for DC functions including antigen presentation and expression of costimulatory molecules that are required for T cell stimulation. We collected BMDCs from C57BL/6 mice to assess the capacity of PNEs in converting immature DCs into mature DCs *in vitro* by monitoring the expression level of costimulatory markers (CD40 and CD80) with flow cytometry analysis (Figure 3A; Figure S8). PNE with copolymerized Pam promoted the stimulation of BMDCs to a similar level as monomeric Pam or the mixture of free LEQ and Pam. Importantly, BMDCs pulsed with PNE(LEQ-Pam) cross-primed the SII-antigen-specific naïve OT-1 CD8⁺ T cells with a greatly enhanced efficiency compared to monomeric SII or LEQ, or the simple mixture of short or long peptides with Pam, assessed by a 5(6)-carboxyfluorescein diacetate *N*-succinimidyl ester (CFSE) dilution assay (Figure 3B,C). We found that the redox-responsiveness of the PNE was crucial for enhanced cross-presentation as nondeg. PNE(LEQ-Pam) exhibited substantially lower efficiency of cross-priming of OT-1 CD8⁺ T cells (Figure S9).

To understand the mechanism by which PNE could promote the cross-presentation of SLPs, we tracked the intracellular trafficking of SLPs delivered by PNE(LEQ-Pam) by labeling the

antigen peptides with Alexa Fluor 647 and monitoring the antigen localization in BMDCs using confocal microscopy (Figure 3D). Upon 24 h of coinubation of BMDCs and PNE(LEQ-Pam), a significant amount of antigens (red) were found dis-localized with endolysosomes stained with LysoTracker (green), and the signal in cytosol was sustained up to 48 h. By contrast, in BMDCs incubated with the mixture of free LEQ and Pam, a majority of the antigens stayed colocalized with endolysosomes, and the fluorescent signal of total intracellular antigens decreased rapidly after a 24 h incubation. Therefore, the responsive PNE facilitated the endosomal escape of the peptide antigens leading to subsequent MHC class I molecule loading and cross-presentation. Endosomal escape of SLPs was likely through the pH-buffering effect of the released cationic peptides and/or the endosomal membrane fusion with the lipopeptides (Pam).^{34,35}

Encouraged by the results showing enhanced LN targeting and cross-presentation of PNE, we next determined the T cell immune response and antitumor activity induced by PNE vaccination *in vivo*. C57BL/6 mice were immunized subcutaneously with one prime (day 0) and 2 boosts (day 14, 28) vaccinations of PNE(LEQ-Pam) (containing 15 nmol of LEQ and 5 nmol of Pam), or the mixture of equivalent doses of LEQ and Pam in the form of solution or emulsion in Montanide (Figure 4A). Peripheral blood mononuclear cells (PBMCs) were collected 1 week after each immunization and stained with

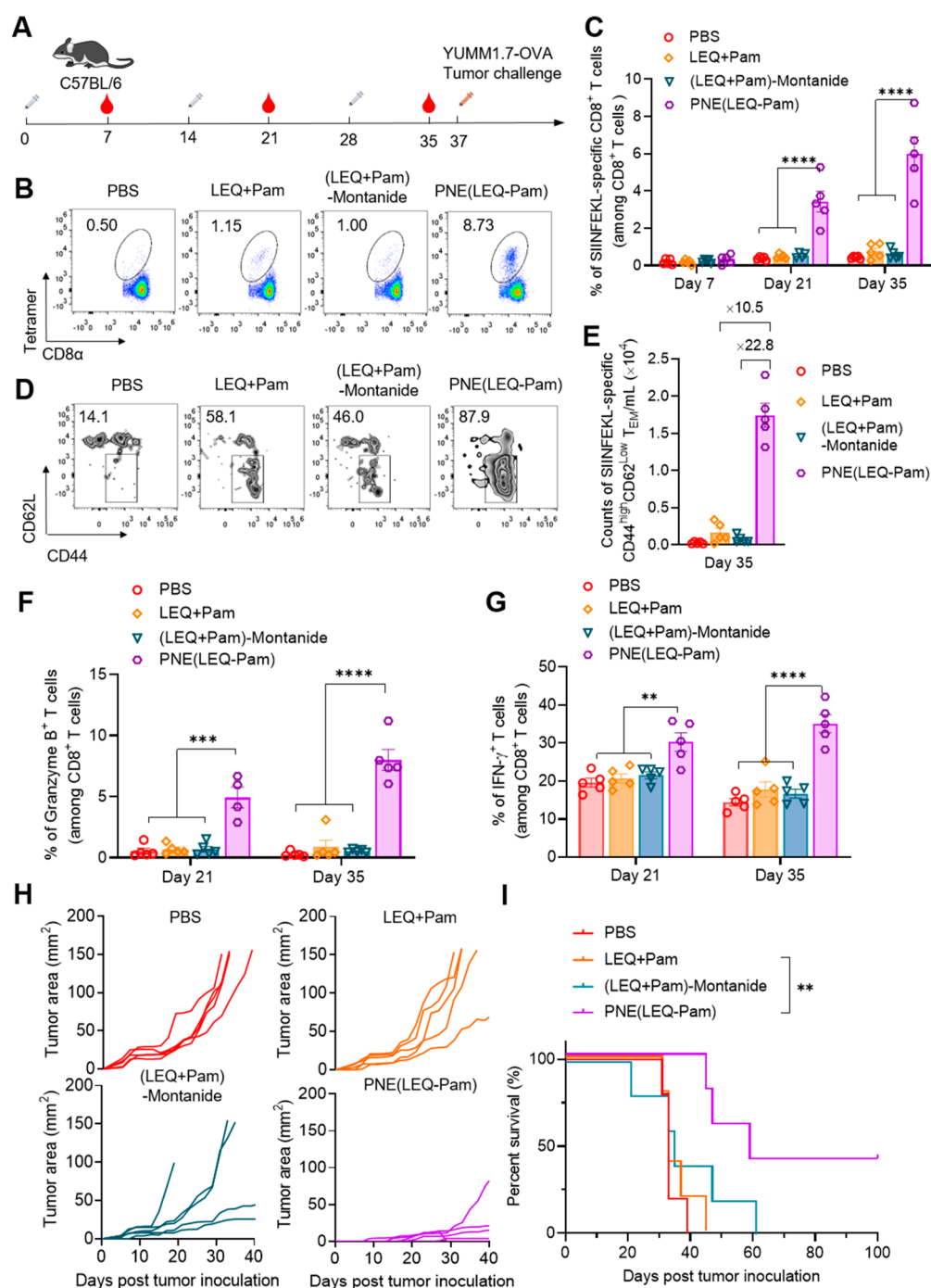


Figure 4. PNE(LEQ-Pam) vaccine elicited potent antigen-specific CD8⁺ T cell response. (A) C57BL/6 mice were vaccinated with PBS, LEQ+Pam, (LEQ+Pam)-Montanide, or PNE(LEQ-Pam) on day 0, 14, and 28. The peripheral blood was collected 7 days after each vaccination. Mice were subcutaneously challenged with YUMM1.7-OVA cells (5×10^5) on day 37 ($n = 5$ independent animals each group). (B) Representative flow cytometry plots showing the frequencies of SII-specific CD8a⁺ T cells from the PBMCs on day 35. (C) Average frequencies of SII-specific CD8⁺ T cells in peripheral blood on day 7, 21, and 35. (D) Representative flow cytometry plots showing the frequencies of CD44^{high}CD62L^{low} T_{EM} cells among SII-specific CD8⁺ T cells. (E) Counts of SII-specific CD8⁺ T_{EM} cells on day 35. The frequencies of Granzyme B⁺ (F) and IFN- γ ⁺ T cells (G) in CD8⁺ T cells in the peripheral blood were measured 7 days after the second and third vaccination by intracellular staining. The data show mean \pm SEM from a representative experiment ($n = 5$). (H) Tumor growth curves of each group in the prophylactic experiment. (I) Survival rate of mice in each group. The statistical analyses between groups were performed by one-way ANOVA for flow cytometry data and Log-rank test for survival curves; * $P < 0.05$; ** $P < 0.01$; *** $P < 0.001$; **** $P < 0.0001$.

SII tetramer to examine the frequency of SII-MHC-I tetramer⁺CD8⁺ T cells. The simple mixture of LEQ and Pam induced a minimum T cell immune response with a mean frequency of SII-specific CD8⁺ T cells close to the background (0.77% SII-specific T cells among CD8⁺ T cells vs 0.44% in

nonimmunized mice) after the second boost; the mixture emulsified in Montanide showed only modest improvement (0.60% SII-specific T cells among CD8⁺ T cells on day 35, Figure 4B,C). In contrast, PNE(LEQ-Pam) vaccine elicited a high frequency (6.00%) of SII-specific CD8⁺ T cells that was 7.8-

and 10-fold higher compared to the mixture of LEQ and Pam in solution and Montanide, respectively (day 35, Figure 4B,C). The majority (87.9%) of the elicited antigen-specific CD8⁺ T cells by PNE(LEQ-Pam) exhibited effector memory phenotype (CD44^{high}CD62^{low}) (Figure 4D). Notably, PNE vaccines remarkably expanded the antigen-specific T_{EM} cells to a number 10.5- and 22.8-fold greater than that of the mixture of LEQ and Pam in solution and Montanide, respectively (day 35, Figure 4E). Importantly, mice immunized with PNEs also showed markedly increased frequency of Granzyme B-secreting CD8⁺ T cells, which was 9.0- and 14.8-fold higher than that in mice immunized with the mixture of LEQ and Pam in solution and Montanide, respectively (Figure 4F), suggesting that PNE vaccination also enhanced the cytotoxicity of CD8⁺ T cells. Furthermore, on average 35.1% of the CD8⁺ T cells in PBMC produced effector cytokines, such as interferon- γ (IFN- γ) (Figure 4G), indicating the increased effector functions. In addition to the model antigen SII, the PNE(ELE-Pam) vaccine against adpgk (Table 1, entry 6), a neoepitope identified in MC38 murine colon adenocarcinoma,³⁶ also exhibited increased antigen-specific CD8⁺ T cell response compared to the mixture of soluble peptide and adjuvant (Figure S10).

The markedly enhanced vaccination efficiency by PNE motivated us to evaluate its antitumor efficacy. The immunized mice were challenged subcutaneously with YUMM1.7-OVA cells (5×10^5), a murine melanoma cell line expressing OVA antigens. Mice immunized with PNE(LEQ-Pam) vaccine showed significantly delayed tumor growth (Figure 4H) and prolonged survival (Figure 4I). Notably, 2 out of 5 mice exhibited durable cures for at least 100 days post-tumor-inoculation. These two survivors maintained 1.90% and 1.35% antigen-specific CD8⁺ T cells in the PBMC which were mostly central memory cells (Figure S11) providing durable protection. In addition, in a more challenging therapeutic setting, C57BL/6 mice were first inoculated with YUMM1.7-OVA tumor cells (5×10^5 cells), followed by multiple vaccinations with PNE or the mixture of equivalent doses of LEQ and Pam in the form of a solution or emulsion in Montanide (Figure S12A). It is notable that mice treated with PNE vaccines exhibited a significantly enhanced capacity in inhibiting tumor growth and extending the survival of treated mice compared to the vaccine of mixed antigen and adjuvant in Montanide (Figure S12B,C).

CONCLUSIONS

In summary, we have demonstrated a responsive PNE as a facile, effective, and versatile vaccine platform for the delivery of peptide neoantigens to enhance personalized cancer immunotherapy. PNE is a highly modular system permitting the copolymerization of peptide antigens and molecular adjuvants of diverse structures and properties, which is a highly desired property as individually identified neoantigens from patients could vastly differ in physicochemical properties. We envision that this new strategy can be readily extended to the codelivery of multiple heterogeneous epitopes in form of SLPs, proteins (e.g., whole tumor cell lysate), or replicon mRNAs/DNAs encoding the neoepitopes. Implementation of various responsive chemistries in the linker-monomer (monomer B) could potentially impart different responsiveness to the PNEs facilitating triggered release of antigens and/or adjuvants by intracellular stimuli including pH change, reactive oxygen species, protease, etc.

Direct assembly of peptide or protein antigens relying on noncovalent assembly^{37–41} or disulfide cross-linking^{42,43} with-

out carriers is actively being pursued as reported in some elegant studies recently. Such “carrier-free” approaches including ours have the unique advantage of minimizing the potential risk of using additional carrier materials whose own immunogenicity and safety profile have to be determined before clinical applications.^{20,44–47} The PNE approach described here based on a highly efficient covalent conjugation of amines in DMSO or aqueous solution does not require the use of any denaturing conditions such as heating and, therefore, showed high promise for the delivery of a wide range of individualized neoepitopes with good compatibility.

ASSOCIATED CONTENT

Supporting Information

The Supporting Information is available free of charge at <https://pubs.acs.org/doi/10.1021/acscentsci.9b01174>.

Additional experimental details, data, and figures including synthetic strategy, PNE preparation and characterizations, *in vitro* and *in vivo* assays, statistical analysis, and safety consideration (PDF)

AUTHOR INFORMATION

Corresponding Author

Li Tang – École Polytechnique Fédérale de Lausanne, Lausanne, Switzerland; orcid.org/0000-0002-6393-982X; Email: li.tang@epfl.ch

Other Authors

Lixia Wei – École Polytechnique Fédérale de Lausanne, Lausanne, Switzerland

Yu Zhao – École Polytechnique Fédérale de Lausanne, Lausanne, Switzerland

Xiaomeng Hu – École Polytechnique Fédérale de Lausanne, Lausanne, Switzerland

Complete contact information is available at: <https://pubs.acs.org/doi/10.1021/acscentsci.9b01174>

Author Contributions

[§]L.W. and Y.Z. are considered cofirst authors. X.H. performed the immunization and antitumor experiments.

Notes

The authors declare the following competing financial interest(s): L.T., L.W., and Y.Z. are inventors on patents related to the technology described in this manuscript.

ACKNOWLEDGMENTS

This work was supported in part by Swiss National Science Foundation (Project grant 315230_173243), the Foundation Pierre Mercier pour la science, ISREC Foundation with a donation from the Bilema Foundation, Novartis Foundation for medical-biological Research (17A058), Swiss Cancer League (KFS-4600-08-2018), and École polytechnique fédérale de Lausanne (EPFL). Y.Z. is a EuroTech Postdoctoral Fellow (The Eurotech Postdoc Programme is cofunded by the European Commission under its framework programme Horizon 2020 (grant agreement 754462)). X.H. is supported by the Chinese Scholarship Council (CSC) (File 201700260266).

REFERENCES

(1) Melero, I.; Gaudernack, G.; Gerritsen, W.; Huber, C.; Parmiani, G.; Scholl, S.; Thatcher, N.; Wagstaff, J.; Zielinski, C.; Faulkner, I.;

Mellstedt, H. Therapeutic vaccines for cancer: an overview of clinical trials. *Nat. Rev. Clin. Oncol.* **2014**, *11* (9), 509–524.

(2) Romero, P.; Banchereau, J.; Bhardwaj, N.; Cockett, M.; Disis, M. L.; Dranoff, G.; Gilboa, E.; Hammond, S. A.; Hershberg, R.; Korman, A. J.; Kvistborg, P.; Melief, C.; Mellman, I.; Palucka, A. K.; Redchenko, I.; Robins, H.; Sallusto, F.; Schenkelberg, T.; Schoenberger, S.; Sosman, J.; Türeci, Ö.; Van der Eynde, B.; Koff, W.; Coukos, G. The human vaccines project: a roadmap for cancer vaccine development. *Sci. Transl. Med.* **2016**, *8* (334), 334ps9.

(3) Ott, P. A.; Hu, Z.; Keskin, D. B.; Shukla, S. A.; Sun, J.; Bozym, D. J.; Zhang, W.; Luoma, A.; Giobbie-Hurder, A.; Peter, L.; Chen, C.; Olive, O.; Carter, T. A.; Li, S.; Lieb, D. J.; Eisenhaure, T.; Gjini, E.; Stevens, J.; Lane, W. J.; Javeri, I.; Nellaiappan, K.; Salazar, A. M.; Daley, H.; Seaman, M.; Buchbinder, E. I.; Yoon, C. H.; Harden, M.; Lennon, N.; Gabriel, S.; Rodig, S. J.; Barouch, D. H.; Aster, J. C.; Getz, G.; Wucherpennig, K.; Neuberger, D.; Ritz, J.; Lander, E. S.; Fritsch, E. F.; Hachohen, N.; Wu, C. J. An immunogenic personal neoantigen vaccine for patients with melanoma. *Nature* **2017**, *547* (7662), 217–221.

(4) Sahin, U.; Derhovanessian, E.; Miller, M.; Kloke, B. P.; Simon, P.; Lower, M.; Bukur, V.; Tadmor, A. D.; Luxemburger, U.; Schrörs, B.; Omokoko, T.; Vormehr, M.; Albrecht, C.; Paruzynski, A.; Kuhn, A. N.; Buck, J.; Heesch, S.; Schreeb, K. H.; Müller, F.; Ortseifer, I.; Vogler, I.; Godehardt, E.; Attig, S.; Rae, R.; Breitkreuz, A.; Tolliver, C.; Suchan, M.; Martic, G.; Hohberger, A.; Sorn, P.; Diekmann, J.; Ciesla, J.; Waksman, O.; Bruck, A. K.; Witt, M.; Zillgen, M.; Rothermel, A.; Kasemann, B.; Langer, D.; Bolte, S.; Diken, M.; Kreiter, S.; Nemecek, R.; Gebhardt, C.; Grabbe, S.; Holler, C.; Utikal, J.; Huber, C.; Loquai, C.; Türeci, O. Personalized RNA mutanome vaccines mobilize poly-specific therapeutic immunity against cancer. *Nature* **2017**, *547* (7662), 222–226.

(5) Carreno, B. M.; Magrini, V.; Becker-Hapak, M.; Kaabinejadian, S.; Hundal, J.; Petti, A. A.; Ly, A.; Lie, W. R.; Hildebrand, W. H.; Mardis, E. R.; Linette, G. P. A dendritic cell vaccine increases the breadth and diversity of melanoma neoantigen-specific T cells. *Science* **2015**, *348* (6236), 803–808.

(6) Yarchoan, M.; Johnson, B. A., 3rd; Lutz, E. R.; Laheru, D. A.; Jaffee, E. M. Targeting neoantigens to augment antitumor immunity. *Nat. Rev. Cancer* **2017**, *17* (4), 209–222.

(7) Hu, Z.; Ott, P. A.; Wu, C. J. Towards personalized, tumour-specific, therapeutic vaccines for cancer. *Nat. Rev. Immunol.* **2018**, *18* (3), 168–182.

(8) Guo, Y.; Lei, K.; Tang, L. Neoantigen vaccine delivery for personalized anticancer immunotherapy. *Front. Immunol.* **2018**, *9*, 01499.

(9) Rosalia, R. A.; Quakkelaar, E. D.; Redeker, A.; Khan, S.; Camps, M.; Drijfhout, J. W.; Silva, A. L.; Jiskoot, W.; van Hall, T.; van Veelen, P. A.; Janssen, G.; Franken, K.; Cruz, L. J.; Tromp, A.; Oostendorp, J.; van der Burg, S. H.; Ossendorp, F.; Melief, C. J. Dendritic cells process synthetic long peptides better than whole protein, improving antigen presentation and T-cell activation. *Eur. J. Immunol.* **2013**, *43* (10), 2554–2565.

(10) Zhang, H.; Hong, H.; Li, D.; Ma, S.; Di, Y.; Stoten, A.; Haig, N.; Gleria, D. K.; Yu, Z.; Xu, X.-N.; McMichael, A.; Jiang, S. Comparing pooled peptides with intact protein for accessing cross-presentation pathways for protective CD8+ and CD4+ T cells. *J. Biol. Chem.* **2009**, *284* (14), 9184–9191.

(11) Kumai, T.; Kobayashi, H.; Harabuchi, Y.; Celis, E. Peptide vaccines in cancer-eld concept revisited. *Curr. Opin. Immunol.* **2017**, *45*, 1–7.

(12) Moyer, T. J.; Zmolek, A. C.; Irvine, D. J. Beyond antigens and adjuvants: formulating future vaccines. *J. Clin. Invest.* **2016**, *126* (3), 799–808.

(13) Bachmann, M. F.; Jennings, G. T. Vaccine delivery: a matter of size, geometry, kinetics and molecular patterns. *Nat. Rev. Immunol.* **2010**, *10* (11), 787–796.

(14) Nuhn, L.; Vanparijs, N.; De Beuckelaer, A.; Lybaert, L.; Verstraete, G.; Deswarte, K.; Lienenklaus, S.; Shukla, N. M.; Salyer, A. C.; Lambrecht, B. N.; Grooten, J.; David, S. A.; De Koker, S.; De Geest, B. G. pH-degradable imidazoquinoline-ligated nanogels for lymph

node-focused immune activation. *Proc. Natl. Acad. Sci. U. S. A.* **2016**, *113* (29), 8098–8103.

(15) Melief, C. J. M.; van Hall, T.; Arens, R.; Ossendorp, F.; van der Burg, S. H. Therapeutic cancer vaccines. *J. Clin. Invest.* **2015**, *125* (9), 3401–3412.

(16) van der Burg, S. H.; Arens, R.; Ossendorp, F.; van Hall, T.; Melief, C. J. M. Vaccines for established cancer: overcoming the challenges posed by immune evasion. *Nat. Rev. Cancer* **2016**, *16* (4), 219–233.

(17) Kovacsics-Bankowski, M.; Rock, K. L. A phagosome-to-cytosol pathway for exogenous antigens presented on MHC Class I molecules. *Science* **1995**, *267* (5195), 243–246.

(18) Kenter, G. G.; Welters, M. J. P.; Valentijn, A. R. P. M.; Lowik, M. J. G.; Berends-van der Meer, D. M. A.; Vloon, A. P. G.; Essahsah, F.; Fathers, L. M.; Offringa, R.; Drijfhout, J. W.; Wafelman, A. R.; Oostendorp, J.; Jan Fleuren, G.; van der Burg, S. H.; Melief, C. J. M. Vaccination against HPV-16 oncoproteins for vulvar intraepithelial neoplasia. *N. Engl. J. Med.* **2009**, *361*, 1838–1847.

(19) Fourcade, J.; Kudela, P.; Andrade Filho, P. A.; Janjic, B.; Land, S. R.; Sander, C.; Krieg, A.; Donnerberg, A.; Shen, H.; Kirkwood, J. M.; Zarour, H. M. Immunization with analog peptide in combination with CpG and montanide expands tumor antigen-specific CD8+ T cells in melanoma patients. *J. Immunother.* **2008**, *31* (8), 781–791.

(20) Kuai, R.; Ochyl, L. J.; Bahjat, K. S.; Schwendeman, A.; Moon, J. J. Designer vaccine nanodiscs for personalized cancer immunotherapy. *Nat. Mater.* **2017**, *16* (4), 489–496.

(21) McLennan, D. N.; Porter, C. J.; Charman, S. A. Subcutaneous drug delivery and the role of the lymphatics. *Drug Discovery Today: Technol.* **2005**, *2* (1), 89–96.

(22) Miller, N. E.; Michel, C. C.; Nanjee, M. N.; Olszewski, W. L.; Miller, I. P.; Hazell, M.; Olivecrona, G.; Sutton, P.; Humphreys, S. M.; Frayn, K. N. Secretion of adipokines by human adipose tissue in vivo: partitioning between capillary and lymphatic transport. *Am. J. Physiol. Endocrinol. Metab.* **2011**, *301* (4), E659–E667.

(23) Supersaxo, A.; Hein, W. R.; Steffen, H. Effect of molecular weight on the lymphatic absorption of water-soluble compounds following subcutaneous administration. *Pharm. Res.* **1990**, *7* (2), 167–169.

(24) Blander, J. M.; Medzhitov, R. Toll-dependent selection of microbial antigens for presentation by dendritic cells. *Nature* **2006**, *440* (7085), 808–812.

(25) Khan, S.; Bijker, M. S.; Weterings, J. J.; Tanke, H. J.; Adema, G. J.; van Hall, T.; Drijfhout, J. W.; Melief, C. J.; Overkleef, H. S.; van der Marel, G. A.; Filippov, D. V.; van der Burg, S. H.; Ossendorp, F. Distinct uptake mechanisms but similar intracellular processing of two different toll-like receptor ligand-peptide conjugates in dendritic cells. *J. Biol. Chem.* **2007**, *282* (29), 21145–21159.

(26) Zom, G. G.; Khan, S.; Britten, C. M.; Sommandas, V.; Camps, M. G.; Loof, N. M.; Budden, C. F.; Meeuwenoord, N. J.; Filippov, D. V.; van der Marel, G. A.; Overkleef, H. S.; Melief, C. J.; Ossendorp, F. Efficient induction of antitumor immunity by synthetic toll-like receptor ligand-peptide conjugates. *Cancer Immunol. Res.* **2014**, *2* (8), 756–764.

(27) Luo, Y.; Friese, O. V.; Runnels, H. A.; Khandke, L.; Zlotnick, G.; Aulabaugh, A.; Gore, T.; Vidunas, E.; Raso, S. W.; Novikova, E.; Byrne, E.; Schlittler, M.; Stano, D.; Dufield, R. L.; Kumar, S.; Anderson, A. S.; Jansen, K. U.; Rouse, J. C. The dual role of lipids of the lipoproteins in trumenba, a self-adjuvanting vaccine against meningococcal meningitis B disease. *AAPS J.* **2016**, *18* (6), 1562–1575.

(28) Cai, H.; Sun, Z. Y.; Chen, M. S.; Zhao, Y. F.; Kunz, H.; Li, Y. M. Synthetic multivalent glycopeptide-lipo-peptide antitumor vaccines: impact of the cluster effect on the killing of tumor cells. *Angew. Chem., Int. Ed.* **2014**, *53* (6), 1699–1703.

(29) Skakuj, K.; Wang, S.; Qin, L.; Lee, A.; Zhang, B.; Mirkin, C. A. Conjugation chemistry-dependent T-cell activation with spherical nucleic acids. *J. Am. Chem. Soc.* **2018**, *140* (4), 1227–1230.

(30) Rudra, J. S.; Banasik, B. N.; Milligan, G. N. A combined carrier-adjuvant system of peptide nanofibers and toll-like receptor agonists potentiates robust CD8+ T cell responses. *Vaccine* **2018**, *36* (4), 438–441.

- (31) Reddy, S. T.; van der Vlies, A. J.; Simeoni, E.; Angeli, V.; Randolph, G. J.; O'Neil, C. P.; Lee, L. K.; Swartz, M. A.; Hubbell, J. A. Exploiting lymphatic transport and complement activation in nanoparticle vaccines. *Nat. Biotechnol.* **2007**, *25* (10), 1159–1164.
- (32) Tang, L.; Yang, X.; Dobrucki, L. W.; Chaudhury, I.; Yin, Q.; Yao, C.; Lezmi, S.; Helfferich, W. G.; Fan, T. M.; Cheng, J. Aptamer-functionalized, ultra-small, monodisperse silica nanoconjugates for targeted dual-modal imaging of lymph nodes with metastatic tumors. *Angew. Chem., Int. Ed.* **2012**, *51*, 12721–12726.
- (33) Bijker, M. S.; van den Eeden, S. J.; Franken, K. L.; Melief, C. J.; van der Burg, S. H.; Offringa, R. Superior induction of anti-tumor CTL immunity by extended peptide vaccines involves prolonged, DC-focused antigen presentation. *Eur. J. Immunol.* **2008**, *38* (4), 1033–1042.
- (34) Wadhwa, M. S.; Collard, W. T.; Adami, R. C.; McKenzie, D. L.; Rice, K. G. Peptide-mediated gene delivery: influence of peptide structure on gene expression. *Bioconjugate Chem.* **1997**, *8*, 81–88.
- (35) Varkouhi, A. K.; Scholte, M.; Storm, G.; Haisma, H. J. Endosomal escape pathways for delivery of biologicals. *J. Controlled Release* **2011**, *151* (3), 220–228.
- (36) Yadav, M.; Jhunjhunwala, S.; Phung, Q. T.; Lupardus, P.; Tanguay, J.; Bumbaca, S.; Franci, C.; Cheung, T. K.; Fritsche, J.; Weinschenk, T.; Modrusan, Z.; Mellman, I.; Lill, J. R.; Delamarre, L. Predicting immunogenic tumour mutations by combining mass spectrometry and exome sequencing. *Nature* **2014**, *515* (7528), 572–576.
- (37) Rudra, J. S.; Tian, Y. F.; Jung, J. P.; Collier, J. H. A self-assembling peptide acting as an immune adjuvant. *Proc. Natl. Acad. Sci. U. S. A.* **2010**, *107* (2), 622–627.
- (38) Chiu, Y. C.; Gammon, J. M.; Andorko, J. I.; Tostanoski, L. H.; Jewell, C. M. Modular vaccine design using carrier-free capsules assembled from polyionic immune signals. *ACS Biomater. Sci. Eng.* **2015**, *1* (12), 1200–1205.
- (39) Qiu, F.; Becker, K. W.; Knight, F. C.; Baljon, J. J.; Sevimli, S.; Shae, D.; Gilchuk, P.; Joyce, S.; Wilson, J. T. Poly(propylacrylic acid)-peptide nanoplexes as a platform for enhancing the immunogenicity of neoantigen cancer vaccines. *Biomaterials* **2018**, *182*, 82–91.
- (40) Qiu, L.; Valente, M.; Dolen, Y.; Jager, E.; Beest, M. T.; Zheng, L.; Figdor, C. G.; Verdoes, M. Endolysosomal-escape nanovaccines through adjuvant-induced tumor antigen assembly for enhanced effector CD8(+) T cell activation. *Small* **2018**, *14* (15), No. e1703539.
- (41) Kramer, K.; Shields, N. J.; Poppe, V.; Young, S. L.; Walker, G. F. Intracellular cleavable CpG oligodeoxynucleotide-antigen conjugate enhances anti-tumor immunity. *Mol. Ther.* **2017**, *25* (1), 62–70.
- (42) Wang, K.; Wen, S.; He, L.; Li, A.; Li, Y.; Dong, H.; Li, W.; Ren, T.; Shi, D.; Li, Y. “Minimalist” nanovaccine constituted from near whole antigen for cancer immunotherapy. *ACS Nano* **2018**, *12* (7), 6398–6409.
- (43) Tsoras, A. N.; Champion, J. A. Cross-linked peptide nanoclusters for delivery of oncofetal antigen as a cancer vaccine. *Bioconjugate Chem.* **2018**, *29* (3), 776–785.
- (44) Luo, M.; Wang, H.; Wang, Z.; Cai, H.; Lu, Z.; Li, Y.; Du, M.; Huang, G.; Wang, C.; Chen, X.; Porembka, M. R.; Lea, J.; Frankel, A. E.; Fu, Y. X.; Chen, Z. J.; Gao, J. A STING-activating nanovaccine for cancer immunotherapy. *Nat. Nanotechnol.* **2017**, *12* (7), 648–654.
- (45) Zhu, G.; Mei, L.; Vishwasrao, H. D.; Jacobson, O.; Wang, Z.; Liu, Y.; Yung, B. C.; Fu, X.; Jin, A.; Niu, G.; Wang, Q.; Zhang, F.; Shroff, H.; Chen, X. Intertwining DNA-RNA nanocapsules loaded with tumor neoantigens as synergistic nanovaccines for cancer immunotherapy. *Nat. Commun.* **2017**, *8* (1), 1482.
- (46) Li, A. W.; Sobral, M. C.; Badrinath, S.; Choi, Y.; Graveline, A.; Stafford, A. G.; Weaver, J. C.; Dellacherie, M. O.; Shih, T. Y.; Ali, O. A.; Kim, J.; Wucherpennig, K. W.; Mooney, D. J. A facile approach to enhance antigen response for personalized cancer vaccination. *Nat. Mater.* **2018**, *17* (6), 528–534.
- (47) Wilson, D. S.; Hirosue, S.; Raczy, M. M.; Bonilla-Ramirez, L.; Jeanbart, L.; Wang, R.; Kwissa, M.; Franetich, J. F.; Broggi, M. A. S.; Diaceri, G.; Quaglia-Thermes, X.; Mazier, D.; Swartz, M. A.; Hubbell, J. A. Antigens reversibly conjugated to a polymeric glyco-adjuvant induce protective humoral and cellular immunity. *Nat. Mater.* **2019**, *18* (2), 175–185.